

Finding confined water in the hexagonal phase of $\text{Bi}_{0.05}\text{Eu}_{0.05}\text{Y}_{0.90}\text{PO}_4 \cdot x\text{H}_2\text{O}$ and its impact for identifying the location of luminescence quencher

R S NINGTHOUJAM

Chemistry Division, Bhabha Atomic Research Centre, Mumbai 400 085, India
Email: nraghu_mani@yahoo.co.in; rsn@barc.gov.in

MS received 1 October 2012; revised 5 February 2013; Accepted 12 February 2013

Abstract. ^1H MAS NMR spectra of $\text{Bi}_{0.05}\text{Eu}_{0.05}\text{Y}_{0.90}\text{PO}_4 \cdot x\text{H}_2\text{O}$ show chemical shift from -0.56 ppm at 300 K to -3.8 ppm at 215 K and another one at 5–6 ppm, which are related to the confined or interstitial water in the hexagonal structure and water molecules on the surface of the particles, respectively. Negative value of the chemical shift indicates that H of H_2O is closer to metal ions (Y^{3+} or Eu^{3+}), which is a source of luminescence quencher. H coupling and decoupling ^{31}P MAS NMR spectra at 300 and 250 K show the same chemical shift (-0.4 ppm) indicating that there is no direct bond between P and H. It is concluded that the confined water is not frozen even at 215 K because of the less number of H-bonding.

Keywords. Confined water; hexagonal structure; luminescence.

PACS Nos 78.55.Hx; 77.67.Bf; 76.60.–k

Recently, we found that water molecules are stable in the pores of hexagonal phase of REPO_4 (RE = rare-earth ion) up to 800°C [1,2]. Now, a question arises as to whether this water molecule is different from normal water or not. In the literature, the decrease of freezing temperature of water in pores of silica gels, zeolites and carbon nanotubes was reported and their importance in applications as well as basic understanding of confined water was discussed [3–8]. Also, the study of confined water molecules is important in chemistry, physics and biology because they are associated in many interface chemistry, protein, lipid, DNA, etc. [9–20].

Can similar behaviour be seen in the hexagonal phase of REPO_4 where there are pore and surface water molecules? Amongst tetragonal, monoclinic and hexagonal structures of REPO_4 , hexagonal structure can have zeolite configuration, in which many pores are available along the c -axis (like a channel) [19]. The proposed zeolite configuration is shown in figure 1. In 2D plane of the hexagonal structure, there is a space of 7.055 \AA in diameter along c -axis (pore), whereas distance between two H atoms in H_2O is less than 2 \AA . Thus, H_2O molecules can occupy the pores. In other phases (tetragonal and

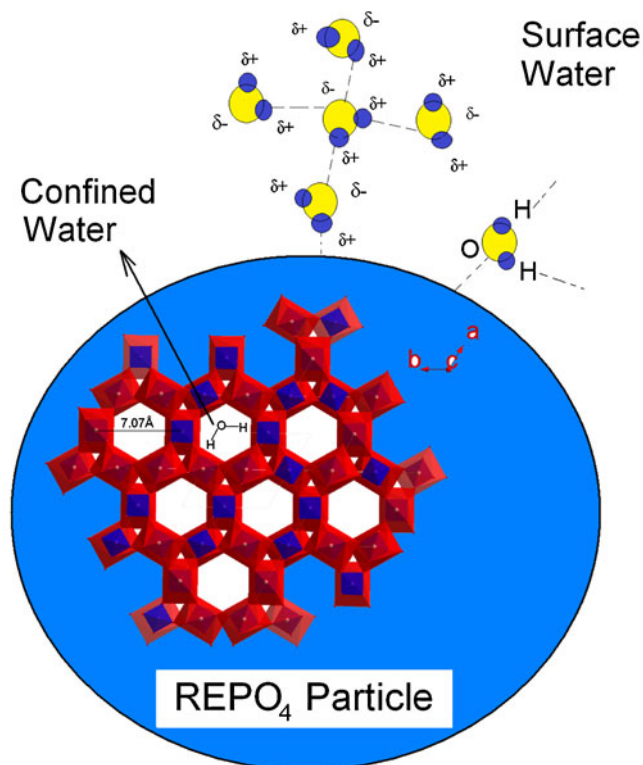


Figure 1. Schematic representation of confined water in pores of the hexagonal structure and surface water in rare-earth phosphate (REPO₄).

monoclinic), there are interstitial sites, but space is very small and water molecules cannot be accommodated [19].

However, to the best of my knowledge, there is no report regarding the NMR technique for determining the presence of H₂O molecules in the pores of hexagonal structure of REPO₄. When REPO₄ is prepared in aqueous medium, a hexagonal structure is formed. On heating at 600–900°C, monoclinic/tetragonal structure is formed. Usually, ratio of water molecule to REPO₄ formula unit is ~0.5:1. On other hand, water molecules on the surface of the particles cannot be avoided when samples are exposed to ambient atmosphere. Water molecules in the pores cannot have enough H-bonding, whereas water molecules present on the surface of the particles can have a maximum of four hydrogen bonds per one molecule of H₂O [5,9], which is shown in figure 1 schematically. In this, can we assume confined water molecule when it is present in the pore? In recent studies of carbon nanotubes (CNs), there are two types of water molecules inside and outside the tube [3–5]. Theoretical model of confined water molecule and experimental results in CNs, water–organic molecules, DNA, lipids and proteins were reported [3–18]. Also, when surface/interface water is in contact with ambient air, it is almost similar to bulk water in terms of the lifetime of the excited O–H bond in 3200–

3500 cm^{-1} [14]. Dynamic behaviour of the frequency of O–H with respect to the nearby surface/hydrophobic/hydrophilic or other H_2O molecule was reported because of energy or charge transfer process using femtosecond midinfrared pulse source [9–18]. A chemical bond such as hydrogen bond, π -bonding and Van-der Waals forces may be present depending on the chemical environment of O–H.

There are many puzzles in luminescence quenching in RE-doped orthophosphates. In our previous study of REPO_4 , luminescence intensity is highly quenched for hexagonal phase compared to that of tetragonal or monoclinic phase [1,2,20]. So far, no report is available on the position of water, i.e., whether it is near PO_4 or $\text{RE}^{3+}/\text{Eu}^{3+}$. The position of water is responsible for the quenching in luminescence. This paper will answer whether the water molecule is near PO_4 or $\text{RE}^{3+}/\text{Eu}^{3+}$.

$\text{Bi}_{0.05}\text{Eu}_{0.05}\text{Y}_{0.90}\text{PO}_4 \cdot x\text{H}_2\text{O}$ ($x < 0.5$) was prepared by heating the as-prepared sample at 500°C . Detailed synthesis procedure is published elsewhere [2]. 0.106 g of $\text{Bi}(\text{NO}_3)_3 \cdot 5\text{H}_2\text{O}$, 0.039 g of Eu_2O_3 and 0.711 g of $\text{Y}_2(\text{CO}_3)_3$ were dissolved in 2 ml of HCl in a 100 ml round bottom flask. Purity of the precursors is $\sim 99.99\%$ (Sigma-Aldrich). Excess acid was removed by evaporation. 10 g of polyethylene glycol (mol. wt. 1000) and 50 ml of glycerol were added to that. It was heated at 50°C for 1 h. 0.5 g of $(\text{NH}_4)_2\text{H}_2\text{PO}_4$ dissolved in 5 ml of glycerol was added to that. The round bottom flask containing the solution was connected with a condenser and heated at 120°C for 2 h. The white precipitate was collected by centrifugation. To remove organic moiety, it was heated at 500°C for 4 h at ambient atmosphere. There were no impurities such as carbon, secondary phase, etc.

Characterization of the samples using X-ray diffraction (XRD), thermogravimetric analysis-differential thermal analysis (TGA-TDA), Fourier transform infra-red (FTIR) and photoluminescence techniques is given in Appendix. NMR data were recorded for the powder samples (i.e., magic angle spinning nuclear magnetic resonance, MAS NMR) using Bruker 500 MHz spectrometer with low temperature facility. The sample holder is zirconia 2.5 mm rotor, in which powder samples were packed and rotor was spun at a frequency of 5–10 kHz. The instrument was fixed at 500 MHz frequency for ^1H NMR. The chemical shift of ^{31}P was referenced to H_3PO_4 (0 ppm). The typical 90° pulse duration and relaxation delay were 4 μs and 2 s, respectively. Number of transients recorded was 512 for each experiment. The data were recorded at 300 and 273–215 K. At 300 K, the fluctuation of temperature is ± 1 K and that of spinning frequency is ± 50 Hz. In 273–215 K, the fluctuation of temperature is ± 5 K and that of spinning frequency is ± 500 Hz. An equilibration time of 10 min was allowed at each temperature before collecting the data.

X-ray diffraction pattern of $\text{Bi}_{0.05}\text{Eu}_{0.05}\text{Y}_{0.90}\text{PO}_4 \cdot x\text{H}_2\text{O}$ ($x < 0.5$) was recorded (see figure A1). It shows the hexagonal phase with lattice parameters $a = 7.106$, $c = 6.470$ Å and $V = 282.94$ Å³. Thermogravimetric analysis of the sample establishes that even sample prepared at 500°C contains surface water molecules after bringing to ambient/room temperature. Such water molecules which are removed below 180°C and bound water molecules are removed at 800°C (figure A2). There is a phase transition at 921°C in the differential thermal analysis (DTA) curve. Above 920°C , the tetragonal phase is formed. Fourier transform infra-red (FTIR) spectrum of this compound is shown in figure A3. The peaks for PO_4 group are observed. The peaks for H_2O are observed at 1616 and 1650 cm^{-1} due to bending vibrations and at 3450 and 3525 cm^{-1} due to stretching

vibrations. The peaks at 1616 and 3525 cm^{-1} are assigned to the confined water because its stretching vibration is more than that of the normal water where there are four hydrogen bonding per one molecule of water. The remaining peaks at 1650 and 3450 cm^{-1} are assigned to the surface water present on the particle. The confined water has less hydrogen bonding than that of the normal/surface water.

The frequencies of O–H can decide the number of hydrogen bonds surrounding the water molecule. If there are four, three and two hydrogen bonds, the IR bands obtained are at 3320 , 3465 and 3585 cm^{-1} , respectively, which are observed on Lamellar Micelles of silica [21]. Based on this, confined water can have two hydrogen bonds per water molecule. Also, there are reports on the interlayered water molecules between NaY_2F_6 and $\text{NH}_4\text{Y}_2\text{F}_7$ (CaF_2 structure) [22] and TiO_6 nanosheet multilayer films [23]. NaY_2F_6 can have vibrations in $3000\text{--}3600\text{ nm}$, due to the presence of water (surface free and bound/interlayered). Peak intensity at 3500 cm^{-1} is much less than 3260 cm^{-1} [22]. It is suggested that the surface water is dominating over interlayered/bound water.

Figure 2a shows the ^1H MAS NMR spectra of $\text{Bi}_{0.05}\text{Eu}_{0.05}\text{Y}_{0.90}\text{PO}_4 \cdot x\text{H}_2\text{O}$ ($x < 0.5$) at 300 , 273 , 250 and 215 K . At the spinning frequency of 10 kHz , we are able to see the asymmetric nature of peak on the left side of the peak at $\sim 5.2\text{ ppm}$ for sample recorded at 300 and 273 K (figures 2b, c). After de-convolution using Lorentzians, two peaks can be separated at -0.56 (hump) and 5.24 (main) ppm at 300 K . At 273 K , peaks at -1.58 (hump) and 5.44 (main) ppm can be observed. At 250 and 215 K , the distinct peak at $\sim -3.8\text{ ppm}$ can be observed in addition to the main peak ($\sim 5\text{--}6\text{ ppm}$). It seems that there is a change in more negative value for peak on the left side of the main peak in the

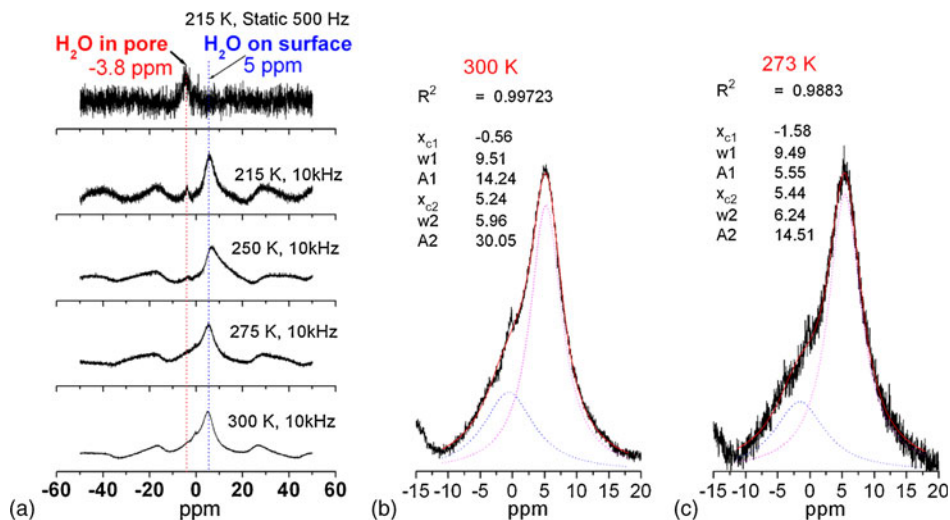


Figure 2. (a) ^1H MAS NMR spectra of $\text{Bi}_{0.05}\text{Eu}_{0.05}\text{Y}_{0.90}\text{PO}_4 \cdot x\text{H}_2\text{O}$ ($x < 0.5$) at 300 , 273 , 250 and 215 K . (b–c) Asymmetric nature of the peak on the left side of the peak at $\sim 5.2\text{ ppm}$ for sample recorded at 300 and 273 K at a spinning frequency of 10 kHz .

spectrum. For static mode at ~ 500 Hz and at 215 K, the main peak disappears but the peak at -3.8 ppm still appears.

When we performed H coupling and decoupling ^{31}P MAS NMR at 300 and 250 K with a fixed spinning frequency of 10 kHz (figure 3a), we have found a peak at -0.4 ppm. It does not change the peak position of P, except the extent of increase of broadening of peak with decreasing temperature (figure 3b). The reported values of isotropic chemical shift of ^{31}P MAS NMR in YPO_4 was -0.9 ppm and chemical shift values of many rare-earth orthophosphates were reported [24,25]. As per [26], the peak at -12.00 ppm corresponds to pure YPO_4 . Chemical shift depends on the paramagnetic environment of ^{31}P and thus their values are different from one compound to another. The probable chemical interactions are: P–O–RE (through direct chemical bonds of covalent or ionic nature), RE–O--- H_2O (through hydrogen bond), P–O--- H_2O (through hydrogen bond) or magnetically dipole interactions. In addition to the main peak corresponding to YPO_4 , paramagnetic peaks could be observed depending on the type of doping ions [26]. Such paramagnetic peaks are explained on the basis of Fermi contact shift and pseudocontact shift. However, we could not observe the paramagnetic peaks in this study with respect to main peak except spinning sidebands (figure A4). It may be due to (1) short relaxation time, (2) 500 MHz is less sensitive to paramagnetic ions and (3) these peaks could not be detected in the background.

The peak at 5–6 ppm in ^1H NMR spectrum corresponds to surface water molecules. Similar value was reported in CdS particles [27]. In carbon nanotubes, free water gives a

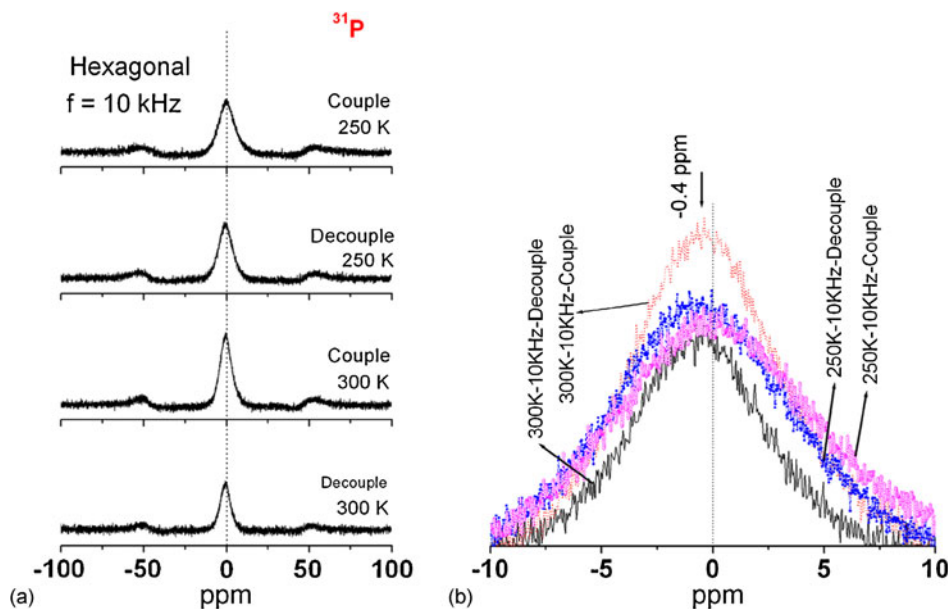


Figure 3. (a) H coupling and decoupling ^{31}P MAS NMR spectra of $\text{Bi}_{0.05}\text{Eu}_{0.05}\text{Y}_{0.90}\text{PO}_4 \cdot x\text{H}_2\text{O}$ ($x < 0.5$) at 300 and 250 K at a fixed spinning frequency of 10 kHz. (b) Expansion of peak near the chemical shift.

chemical shift at 12 ppm [5]. The shift of the peak from -0.56 ppm at 300 K to -3.8 ppm at 215 K may be due to the confined water in the pores or interstitial water in the hexagonal structure. From H coupling and decoupling ^{31}P MAS NMR, it is concluded that there is no direct bond between P and H. The negative value in chemical shift in ^1H NMR indicates that H is close to the metal ion ($\text{Y}^{3+}/\text{Bi}^{3+}/\text{Eu}^{3+}$).

The ^1H MAS NMR spectra recorded at static mode (~ 500 Hz) and at different temperatures are shown in figure A5 for comparison. At 300 K, we can see a peak at 2.5 ppm, corresponding to the surface water, but this value is slightly less than that taken at 10 kHz frequency. There is small hump at the negative side, which may be related to the pore water. Since the number of pore water molecules is much less than the surface water molecules, the main peak corresponding to surface water dominates the peak corresponding to pore water. When temperature decreases to 273 K, the main peak at 2.5 ppm decreases drastically because of the frozen surface water and only peak corresponding to the pore water is observed. When temperature goes to 250 or 215 K, a distinct peak corresponding to the pore at -3.8 ppm is observed.

Here, water molecule present in interstitial/pore may have a maximum of one hydrogen bonding with neighbouring water molecule since there is one water molecule per two formula units of YPO_4 . However, H_2O can have Van-der Waals interaction/hydrogen bonding with AO_9 unit ($\text{H}-\text{O}-\text{H}---\text{O}-\text{A}-\text{O}$ or $\text{H}-\text{O}-\text{H}---\text{A}-\text{O}$ where $\text{A} = \text{Y}^{3+}/\text{Bi}/\text{Eu}^{3+}$).

The typical photoluminescence (PL) spectra of $\text{Bi}_{0.05}\text{Eu}_{0.05}\text{Y}_{0.90}\text{PO}_4 \cdot x\text{H}_2\text{O}$ prepared at 500 and 900°C are shown in figure A6. Luminescence intensity is improved significantly for the sample heated at 900°C compared to the sample heated at 500°C . This improved luminescence is due to the removal of water molecule present in the pores of the hexagonal phase along the c -axis. The quenching of luminescence in the hexagonal phase of Ce^{3+} or Bi^{3+} co-doped $\text{YPO}_4:\text{Eu}$ (REPO_4) even heated samples up to 700°C is high due to the presence of water molecules [1,2]. Samples prepared at different solvents are also found to show different luminescence intensities in our study. Luminescence intensity of hexagonal phase is highly quenched, whereas that of monoclinic or tetragonal phase is high. From NMR study, we can see that confined water is closer to YO_8 or EuO_8 and far from PO_4 group. Because of this, luminescence intensity is quenched in the hexagonal phase of REPO_4 . In the present study, we cannot give exact lifetime values of ^{31}P when water is in the pore or/and surface of the particle.

There are a few reports on the enhancement of luminescence intensity when there are more water molecules in the samples ($\text{TiO}_2:\text{Eu}^{3+}$ and $\text{NaY}_2\text{F}_6:\text{Eu}^{3+}$) prepared at low pH ($= 2-7$) [22,23] and even at high humidity. It is explained that this is due to the increase of crystal field environment on Eu^{3+} with H_2O molecules and $\text{F}^-/\text{O}^{2-}/\text{OH}^-$ ions as ligands. In my opinion, if H_2O is linked to Eu^{3+} as ligand, luminescence intensity will decrease because second and third overtones of O-H frequency/energy can match with gap between ground and excited states of Eu^{3+} ($E_{\text{gap}} = {}^5\text{L}_6, {}^5\text{D}_j-{}^7\text{F}_j$) thereby multiphonon relaxation will be high. Non-radiative rate will be more if water molecules surrounding Eu^{3+} increases. This can be confirmed by the exchange of H_2O with D_2O (isotope effect) [1,2]. Some structure related changes, defects (hole/electron trap) and protonation (H_3O^+) and even reduction of Eu^{3+} to Eu^{2+} to some extent in different pH can occur. This was not discussed in [22,23]. This has to be further characterized by X-ray photoelectron spectroscopy (XPS), electron paramagnetic resonance (EPR), Mössbauer spectroscopy techniques, etc. In our previous work [28], $\text{TiO}_2:\text{Eu}^{3+}$ was

converted to $\text{Eu}_2\text{T}_2\text{O}_7$ on annealing. The former has high luminescence intensity for Eu^{3+} , whereas the latter has very weak luminescence intensity. This is related to the structure related change where Eu^{3+} can have different symmetry environments. Also, there are reports on the creation of defects (hole/electron trap) and protonation (H_3O^+) in

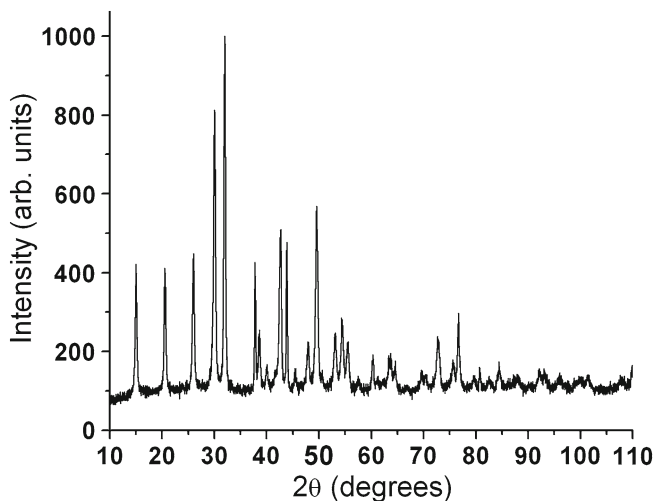


Figure A1. XRD pattern of $\text{Bi}_{0.05}\text{Eu}_{0.05}\text{Y}_{0.90}\text{PO}_4 \cdot x\text{H}_2\text{O}$ ($x < 0.5$) prepared at 500°C .

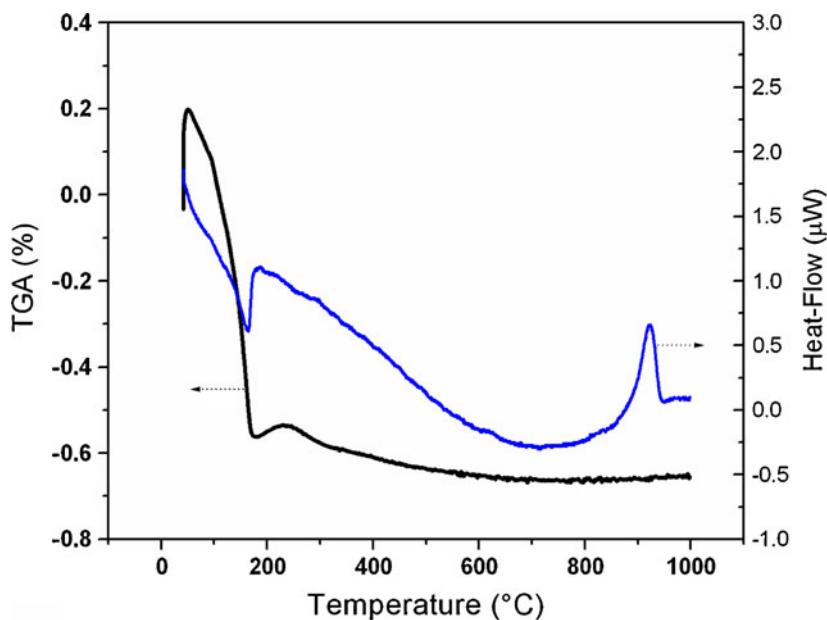


Figure A2. TGA and DTA curves of $\text{Bi}_{0.05}\text{Eu}_{0.05}\text{Y}_{0.90}\text{PO}_4 \cdot x\text{H}_2\text{O}$ ($x < 0.5$) prepared at 500°C .

different pH and environment (ambient atmosphere, O₂, N₂) in silica/silanols [21,29,30]. This leads to changes in luminescence intensity in the blue and green regions [29,30].

In conclusion, the free water is observed on the surface of the particles and confined water is observed in the pores or interstices of the hexagonal structure of orthophosphate. Luminescence quenching in hexagonal REPO₄ phase is due to the confined water, which is closer to the metal ion (Y³⁺/Bi³⁺/Eu³⁺) and far from the PO₄ group.

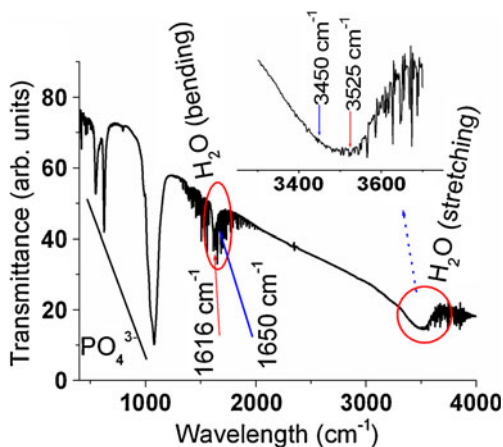


Figure A3. FTIR spectrum of Bi_{0.05}Eu_{0.05}Y_{0.90}PO₄·xH₂O ($x < 0.5$) prepared at 500°C.

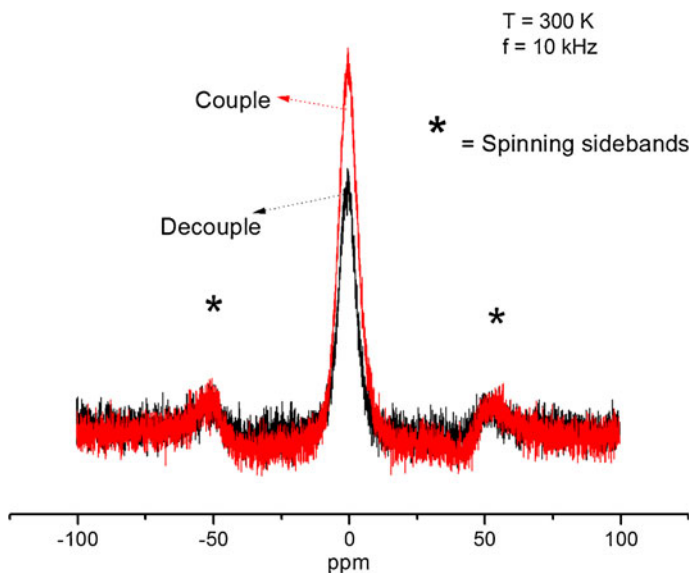


Figure A4. H coupling and decoupling ³¹P MAS NMR spectra of Bi_{0.05}Eu_{0.05}Y_{0.90}PO₄·xH₂O ($x < 0.5$) prepared at 500°C. Data were recorded at 300 K and 10 kHz.

Acknowledgement

The author is grateful to Dr S Srivastava, Mr M Naik, Ms M Joshi and Mr D Jadhav, National Facility for High Field NMR, Mumbai, India for their extensive help during the experiments.

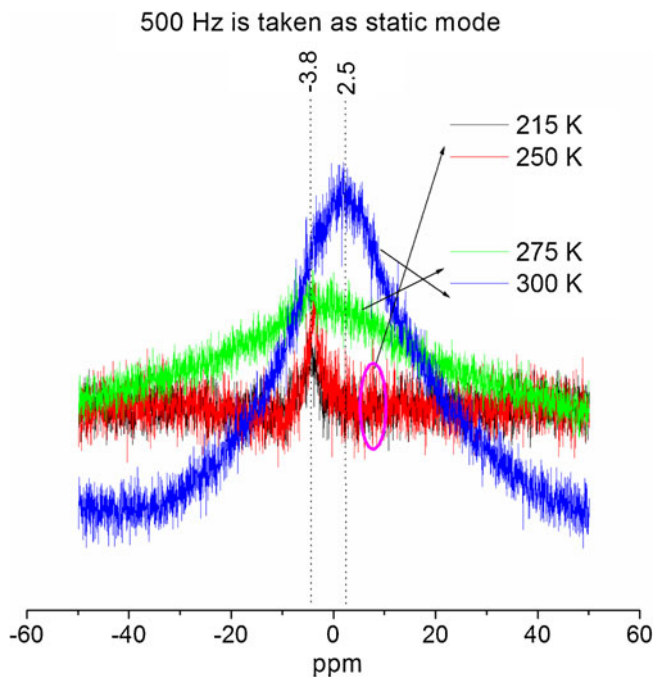


Figure A5. Static ^1H MAS NMR spectra of $\text{Bi}_{0.05}\text{Eu}_{0.05}\text{Y}_{0.90}\text{PO}_4 \cdot x\text{H}_2\text{O}$ ($x < 0.5$) prepared at 500°C (recorded at different temperatures).

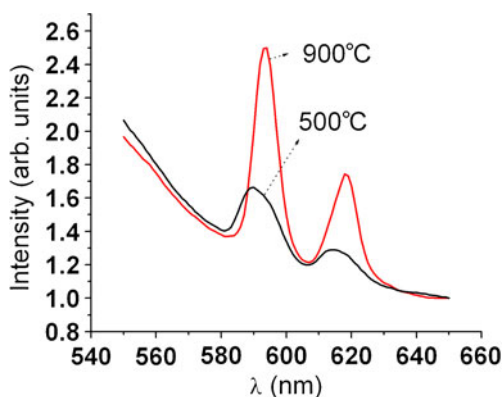


Figure A6. Photoluminescence spectra of $\text{Bi}_{0.05}\text{Eu}_{0.05}\text{Y}_{0.90}\text{PO}_4$ prepared at 500 and 900°C .

Appendix: XRD, FTIR, TGA-DTA and PL characterization techniques

The sample was characterized by the following methods: X-ray diffraction (XRD) patterns were recorded by Inel X-ray diffractometer EQUINOX 1000. Fourier transform infrared (FTIR) spectrum was recorded by FT-IR spectrometer (Bomem MB 102). Thermogravimetric and differential thermal data of sample prepared at 500°C were recorded by TGA-DTA instrument (SETARAM 92-16.18). Weight changes are due to the water content in the sample. Photoluminescence (PL) emission spectra were carried out by Hitachi F-4500 fluorescence spectrometer having a 150 W Xe lamp as the excitation source.

References

- [1] M N Luwang, R S Ningthoujam, S K Srivastava, Jaganath and R K Vatsa, *J. Am. Chem. Soc.* **132**, 2759 (2010)
- [2] M N Luwang, R S Ningthoujam, S K Srivastava and R K Vatsa, *J. Am. Chem. Soc.* **133**, 2998 (2011)
- [3] K Koga, G T Gao, H Tanaka and X C Zeng, *Nature* **412**, 802 (2001)
- [4] G Hummer, J C Rasaiah and J P Noworyta, *Nature* **414**, 188 (2001)
- [5] S Ghosh, K V Ramanathan and A K Sood, *Europhys. Lett.* **65**, 678 (2004)
- [6] V V Chaban and O V Prezhdo, *ACS Nano* **5**, 5647 (2011)
- [7] S Ayyappan, N Suryaprakash, K V Ramanathan and C N R Rao, *J. Porous Mater.* **6**, 5 (1999)
- [8] J H Strange and M Rahman, *Phys. Rev. Lett.* **71**, 3589 (1993)
- [9] K Bhattacharyya, *Acc. Chem. Res.* **36**, 95 (2003)
- [10] A A Vartia and W H Thompson, *J. Phys. Chem. B* **116**, 5414 (2012)
- [11] S Roy and B Bagchi, *J. Phys. Chem. B* **116**, 2958 (2012)
- [12] J A McGuire and Y R Shen, *Science* **313**, 1945 (2006)
- [13] J J Gilijamse, A J Lock and H J Bakker, *Proc. Natl. Acad. Sci.* **102**, 3202 (2005)
- [14] M Smits, A Ghosh, M Sterrer, M Müller and M Bonn, *Phys. Rev. Lett.* **98**, 098302 (2007)
- [15] D E Moilanen, I R Piletic and M D Fayer, *J. Phys. Chem. C* **111**, 8884 (2007)
- [16] V V Volkov, D J Palmer and R Righini, *J. Phys. Chem. B* **111**, 1377 (2007)
- [17] R K Campen, T T M Ngo, M Sovago, J-M Ruyschaert and M Bonn, *J. Am. Chem. Soc.* **132**, 8037 (2010)
- [18] J A Mondal, S Nihonyanagi, S Yamaguchi and T Tahara, *J. Am. Chem. Soc.* **134**, 7842 (2012)
- [19] A C L Mooney, *Acta Crystallogr.* **3**, 337 (1957)
- [20] G Phaomei, W R Singh and R S Ningthoujam, *J. Lumin.* **131**, 1164 (2011)
- [21] S Banerjee, H Ghosh and A Datta, *J. Phys. Chem. C* **115**, 19023 (2011)
- [22] P Ghosh and A Patra, *J. Phys. Chem. C* **112**, 3223 (2008)
- [23] Y Matsumoto, U Unal, Y Kimura, S Ohashi and K Izawa, *J. Phys. Chem. B* **109**, 12748 (2005)
- [24] G L Turner, K A Smith, R J Kirpatrick and E Oldfield, *J. Magn. Resonance* **70**, 408 (1986)
- [25] M Bose, M Bhattacharya and S Ganguli, *Phys. Rev. B* **19**, 72 (1979)
- [26] A C Palke and J F Stebbins, *American Mineralogist* **96**, 1343 (2011)
- [27] V Ladizhansky, G Hodes and S Vega, *J. Phys. Chem. B* **104**, 1939 (2000)
- [28] R S Ningthoujam, V Sudarsan, R K Vatsa, R M Kadam, Jagannath and A Gupta, *J. Alloys Compounds* **486**, 864 (2009)
- [29] S Banerjee, S Maity and A Datta, *J. Phys. Chem. C* **115**, 22804 (2011)
- [30] S Banerjee and A Datta, *Langmuir* **26**, 1172 (2010)